**Interactive comment on "Improvement in cloud retrievals from VIIRS through the use of infrared absorption channels constructed from VIIRS-CrIS data fusion" by Yue Li et al.**

Anonymous Referee #1
Received and published: 25 March 2020

The present manuscript describes and validates the improvement of cloud retrievals from the VIIRS instrument on board of Suomi-NPP platform using radiances from CrIS hyperspectral instrument on board of the same platform.

The authors, using a fusion methodology, extracted broadband channel information from CrIS spectrally resolved measurements to simulate MODIS channels around 15 micron and 6.7 micron. In this way they can apply methodologies developed for MODIS to VIIRS that don't cover these spectral bands for cloud detection and retrieval. This improvement is been validated with CALIPSO dataset.

The manuscript topic is for sure appropriate for the Journal but in the present form has some incompleteness that should be fixed before publication. Incompleteness can be identified divided into two main topics: Hyperspectal instruments and Validation.

- Regarding hyperspectral instruments as I said, in this work the authors use the spectrally resolved measurements of CrIS to simulate moderate resolution channels. In doing this the authors omitted to describe and acknowledge the great diagnostic power inside the spectral resolution and coverage of instruments like CrIS. For a reader who is not an expert in the field, it might appear that CrIS (and all the hyperspectral instruments) is a less accurate instrument than VIIRS because it has a worse spatial resolution. As an example, consider sentence at lines 15-21 of page 2 and lines 1-5 of page 3. It seems that CrIS has channels at 15 and 6.7 micron, missing in VIIRS instrument, but with degraded spatial resolution. I think that the authors should spend a sentence to indicate the peculiarities of hyperspectral instruments and add a figure showing a typical CrIS measurement in comparison with the spectral coverage of the channels used in the methodology described in the manuscript. Moreover I wish to recall that already 15 years ago it has been shown that with hyperspectral observation alone in the atmospheric window between 800-900 cm−1 is possible to detect and classify clouds. The authors can find an example in the following papers doi:10.1364/AO.41.000965 and doi:10.1016/S0022-4073(02)00083-3.

**Response: We made changes to better describe CrIS, which is a highly calibrated hyperspectral sounder. As the reviewer notes, the spatial resolution is much larger than that for VIIRS. Our methodology bridges this gap between the two sensors.**

**For the figure showing a typical CrIS measurement in comparison with channels used in this study, please refer to Fig. 1 in Weisz et al. (2017):**

**Weisz, E., B. A. Baum, and W. P. Menzel, 2017: Construction of high spatial resolution narrowband infrared radiances from satellite-based imager and sounder data fusion. J. Appl. Remote Sens. 11 (3), 036022, doi: 10.1117/1.JRS.11.036022**

**We also included discussion of using the sounder for cloud detection and added the two papers in the Reference. New text reads "Previous studies detected the presence of clouds and retrieved cloud top height directly from sounder data (Masiello et al. 2002, 2003; Susskind et al. 2003; Li et al. 2005; Kahn et al. 2007)".**

• About the validation, I have some doubts regarding the spatial distance between VIIRS and CALIPSO used for the colocation. While on the one hand I can imagine that a distance of less than 4◦ can reduce the concomitances between the two instruments, on the other a distance of 200 kilometers make the difference in spatial resolution between VIIRS and CrIS practically not appreciable. Probably a sentence that best justifies this choice is necessary. Also in relation to the results of the validation itself.

**Response: In addition to the spatial distance constraint, we also adopt other constraints to ensure collocations are appropriate between the two satellites. These include time differences, a sensor zenith threshold, a parallax correction, and minimum counts of collocations. This was also described in Heidinger et al. (2019) where the same collocation technique was used.**

**In replying to the reviewer's concerns, we ran collocations using a tighter spatial difference of 0.1 degree and presented the results for NOAA-20 below. It can be seen that while the counts decrease, the bias, standard deviation, and mode do not vary much compared to Table 5.**

**As suggested, we have added discussion as follows: "This approach allows maximum collocations between the two sensors, particularly in the polar regions. Though a large spatial distance is used, nearly all collocations (>99% globally) occur within 0.5° and about 60% of collocations are within 0.1°. We also note that use of tighter temporal and spatial thresholds does not impact the results significantly."**

**Similar as Table 5, but using collocation with a spatial difference within 0.1 degree.**

| Emissivity | | Counts | Bias (km) | Standard Deviation (km) | Mode (km) |
|---|---|---|---|---|---|
| 0 to 0.4 | No fusion | 19043 | -2.27 | 1.98 | -2.75 |
| | With fusion | | -1.99 | 1.77 | -2.25 |
| 0.4 to 0.8 | No fusion | 5578 | -1.91 | 1.51 | -1.75 |
| | With fusion | | -1.47 | 1.20 | -1.25 |
| 0.8 to 1.0 | No fusion | 73874 | -1.12 | 1.11 | -1.25 |
| | With fusion | | -1.04 | 1.07 | -1.25 |

• Page 2. Line 19. As I said before, CrIS has not only channels MODIS-like at 6.7 and 15 microns, but it covers the spectral ranges that MODIS cover with two channels with thousand channels.

**Response: We added the following text to the introduction: "In general, a sounding sensor is used for retrieving accurate atmospheric temperature and moisture profiles based on its hyperspectral coverage but at a lower spatial resolution than an imager such as VIIRS. CrIS takes measurements at 1305 wavelengths from 3.92-µm to 15.38-µm. The products from the CrIS sounder show significant enhancement over NOAA's legacy HIRS sensors."**

• Page 4. Line 11. Remove absorption before channel.

**Response: Done**

• Page 4. Line 19. The step (b) of the fusion method is not clear. The convolved sounder radiances are already at coarser spatial resolution. In the text it seems that the authors further degraded spatial resolution. Please clarify.

**Response: The convolved sounder radiances are derived for each CrIS field of view (FOV), i.e., at the CrIS native resolution. The basis of our technique is to derive a relationship between the imager 11/12-µm radiances and the average of the imager 11/12-µm pixel radiances within a given CrIS FOV. We do not degrade the CrIS spatial resolution further in this step, but simply average the VIIRS 11/12-µm radiances for all the pixels that lie within each of the CrIS FOVs. This is simply part of the k-d tree search methodology for determining how to best select the CrIS FOVs that should be used for each of the VIIRS**

**pixels to construct the IR absorption band radiances. For more details, please refer to Weisz et al. (2017).**

• Page 6. Line 16. Please insert a reference to the ACHA algorithm. If not, please place here the reference to the ATBD now at Page 7, line 2)

**Response: As suggested, we moved the reference to the ATBD to where ACHA first appeared.**

For these reasons I suggest to accept this manuscript subject to minor but necessary revisions.

**Interactive comment on "Improvement in cloud retrievals from VIIRS through the use of infrared absorption channels constructed from VIIRS-CrIS data fusion" by Yue Li et al.**

Anonymous Referee #2
Received and published: 17 April 2020

General comments: Retrieval of cloud-top properties with the Visible Infrared Imaging Radiometer Suite (VIIRS) could be more challenging than its predecessor MODIS, because of the lack of water vapor and CO2 bands in thermal infrared region. This paper "Improvement in cloud retrievals from VIIRS through the use of infrared absorption channels constructed from VIIRS-CrIS data fusion" by Li et al. demonstrated that by leveraging fusion water vapor and CO2 bands from high-spectral resolution instrument CrIS, VIIRS cloud retrievals, including cloud mask, cloud thermodynamic phase, and cloud-top height are generally improved. This paper also shows that those fusion bands have a big boost in the accuracies of cloud mask/phase algorithm at high latitude. By including the extra fusion bands, cloud-top height retrieval is also improved with lower biases and uncertainties, in particular for those optically thin cirrus clouds with emissivity less than 0.8.

This paper is well organized and written. One of my major concerns is that the authors should give more details about the comparisons between VIIRS retrievals and CALIPSO/CALIOP. Furthermore, to highlight the importance of those absorptive fusion bands, it could be worth to check day/night samples separately.
**Response: We appreciate your comments and address specific comments as noted below.**

**Please note that we studied day/night samples separately for cloud mask, phase and height. Results for cloud mask are presented in response to Comment 7. For cloud phase, the general conclusion is similar and the primary difference between day and night is detecting more water phase clouds during day because of an additional test by the VIIRS 1.6um channel, which also results in slightly larger increase in the percentage of correctly identified ice phase clouds compared to nighttime when fusion channels are used. For cloud height products, since only IR channels are used in ACHA and cloud phase is matched in the validation, no obvious differences are observed. Relevant discussions have been added to the manuscript.**

Specific comments:
1. Line 10, Page 7: What the 13.3 channel is not used in the cloud mask detection?
**Response: The cloud mask team led by one of the coauthors here, Dr. Andrew Heidinger, conducted cloud detection tests using various spectral channels. It was found that adding**

**the 13.3um channel did not help as much as the 6.7um channel. For the way our cloud mask is constructed, one doesn't need both channels.**

2. Line 15 Page 7: Figures 7 and 8 in Wang et al. 2016 [doi.org/10.1002/2015JD024526] shows the importance of 13.3 and 6.7 channels for difference cases.
**Response: We have revised the sentence "It is difficult to explain definitively the information content available in each of these IR bands so the approach is to test their impact on ice cloud height retrievals..." Now it reads "Previous studies explored spectral band information useful for cloud property retrievals by computing the Shannon information content (L'Ecuyer et al. 2006, Wang et al. 2016). The approach used here is to test their impact on ice cloud height retrievals through comparison with another cloud height product."**

3. Line 3, Page 9: I think a 4 degree difference is too large for cloud comparisons. Do you mean 4 km?
**Response: This has been addressed in response to Referee #1's comment.**

4. Line 20, Page 9: How do you define pixel-level cloud fraction here, please clarify.
**Response: We added discussion to clarify how we define pixel level cloud fraction: "When a cloud layer is detected by CALIPSO/CALIOP, the pixel is classified as cloudy. Neighboring pixels along the path are included and the cloud fraction is defined by computing the ratio between the number of cloudy pixels and the total number of pixels."**

5. Line 2, Page 10: Could you please give the pixel fraction that CALIOP COTs are less than 0.03?

**Response: A table is shown below of counts and fraction of CALIOP COTs less than 0.03. We added a sentence as follows: "The fraction of the sub-visible clouds is less than 4% from a global perspective and less than 3% in the polar regions."**

| | | **Sample Size COT < 0.3** | **Sample Size All** | **Ratio** |
|---|---|---|---|---|
| **S-NPP** | **Global** | **217983** | **6091230** | **0.036** |
| | **60°N to 60°S** | **176734** | **4384193** | **0.040** |
| | **Arctic** | **16968** | **853006** | **0.020** |
| | **Antarctic** | **24281** | **854031** | **0.028** |
| **NOAA-20** | **Global** | **73869** | **2328596** | **0.032** |
| | **60°N to 60°S** | **58975** | **1645684** | **0.036** |
| | **Arctic** | **10374** | **329702** | **0.031** |
| | **Antarctic** | **4520** | **353210** | **0.013** |

6. Line 3, Page 10: And it would be helpful if you can provide the cloudy and clear fractions in Table 2.

**Response: We added the numbers of cloud fractions from both sensors to Table 2 and the following discussion: "In terms of total cloud fraction, as expected, VIIRS tends to report a lower cloud fraction than CALIOP. CALIOP has a better detection sensitivity to optically thin clouds, and global cloud fractions reported from the two sensors are in agreement when the minimum cloud optical thickness is set between 0.6 and 0.7. The global values do not necessarily become more closely aligned with CALIOP when a fusion channel is used. However, the use of a fusion channel results in a much larger impact in the polar regions, as will be shown in Figure 1."**

7. Line 19, Page 10: This is true. However, the authors could apply the same comparison to nighttime pixels to highlight the importance of water vapor and CO2 channels.

**Response: We are unsure if the reviewer is referring to this sentence "This is unsurprising since the cloud mask algorithm performs fairly well for a snow-free surface...". As noted, the cloud mask algorithm is not using the CO2 channels. We are computing the validation of cloud mask detection separating day and night as requested below. Note that we used a solar zenith angle threshold of 85 degrees to separate day and night, and discarded pixels that do not have a valid solar zenith angle.**

**Daytime Only**

| | | Sample Size | | Correct Detection | Missed Cloud | False Detection |
|---|---|---|---|---|---|---|
| S-NPP | Global | 2899130 | Fusion | 82.9 | 13.1 | 3.9 |
| | | | No Fusion | 82.4 | 13.6 | 3.9 |
| | 60°N to 60°S | 2154403 | Fusion | 84.3 | 12.5 | 3.1 |
| | | | No Fusion | 84.1 | 12.8 | 3.1 |
| | Arctic | 469177 | Fusion | 77.4 | 15.0 | 7.6 |
| | | | No Fusion | 75.5 | 16.7 | 7.8 |
| | Antarctic | 275550 | Fusion | 80.9 | 14.7 | 4.4 |
| | | | No Fusion | 80.7 | 15.2 | 4.1 |

| | | | | | | |
|---|---|---|---|---|---|---|
| **NOAA-20** | **Global** | **1098695** | **Fusion** | **84.4** | **12.5** | **3.1** |
| | | | **No Fusion** | **83.9** | **13.1** | **3.0** |
| | **60°N to 60°S** | **799995** | **Fusion** | **84.8** | **12.1** | **3.1** |
| | | | **No Fusion** | **84.6** | **12.4** | **3.1** |
| | **Arctic** | **14939** | **Fusion** | **84.9** | **10.0** | **5.1** |
| | | | **No Fusion** | **80.9** | **11.4** | **7.7** |
| | **Antarctic** | **283761** | **Fusion** | **83.3** | **13.8** | **2.8** |
| | | | **No Fusion** | **82.2** | **15.4** | **2.4** |

**Nighttime Only**

| | | **Sample Size** | | **Correct Detection** | **Missed Cloud** | **False Detection** |
|---|---|---|---|---|---|---|
| **S-NPP** | **Global** | **2974117** | **Fusion** | **83.6** | **11.9** | **4.5** |
| | | | **No Fusion** | **82.6** | **12.0** | **5.4** |
| | **60°N to 60°S** | **2053056** | **Fusion** | **87.2** | **8.8** | **4.0** |
| | | | **No Fusion** | **87.1** | **8.7** | **4.2** |
| | **Arctic** | **366861** | **Fusion** | **76.3** | **16.0** | **7.7** |
| | | | **No Fusion** | **73.7** | **17.0** | **9.3** |
| | **Antarctic** | **554200** | **Fusion** | **75.3** | **20.5** | **4.2** |
| | | | **No Fusion** | **71.8** | **21.0** | **7.2** |

| | | | | | | |
|---|---|---|---|---|---|---|
| **NOAA-20** | **Global** | **1156032** | **Fusion** | **81.2** | **13.7** | **5.1** |
| | | | **No Fusion** | **79.6** | **13.4** | **7.0** |
| | **60°N to 60°S** | **786714** | **Fusion** | **86.2** | **9.4** | **4.4** |
| | | | **No Fusion** | **86.1** | **9.2** | **4.7** |
| | **Arctic** | **304389** | **Fusion** | **66.7** | **25.7** | **7.5** |
| | | | **No Fusion** | **60.9** | **25.0** | **14.0** |
| | **Antarctic** | **64929** | **Fusion** | **89.1** | **8.8** | **2.1** |
| | | | **No Fusion** | **88.2** | **10.0** | **1.8** |

8. Table 2: What's the reason that the no fusion cloud mask retrievals are so different between NOAA-20 and SNPP in Arctic (e.g., 74.7% vs. 61.9%)?
**Response: The data used for NOAA-20 and SNPP in this study are from different seasons, so this could be playing a part. The SNPP data are from April and October 2018, while NOAA-20 data are from January 2019. Given the limited amount of data processed for this study, we need to further investigate this difference more closely.**

9. Section 3.2, Page 12: How do you deal with multi-level clouds and mixed-phase cloud? Did you use the uppermost cloud layer phases from CALIOP, in multiple cloudlayer cases? Please give more details.
**Response: CLAVR-x does not retrieve mixed-phase cloud. There is some logic for discriminating the presence of multilayered clouds (primarily optically thin ice clouds overlying a lower-level liquid water cloud), and these are treated as ice phase in this study. We note that the uppermost cloud layer phase from CALIOP in multilayer cases is used.**

10. Line 11, Page 16: In Figure 5, it is interesting that the fusion cloud-top heights (SNPP) are more negatively biased than no fusion heights in Antarctic. Do you have any speculation? I don't find the same feature in Figure 7 for NOAA-20.
**Response: The bias is small in the Antarctic, and we are not sure what caused this behavior. We need to process much more data over seasons to determine whether this is caused by a relatively high surface elevation or some other factor.**

11. Line 13, Page 22: Do you think it's due to artifacts of fusion bands? Since Figure 8c shows that near north pole, passive cloud-top height with fusion bands are higher than Lidar.

**Response: There is an indication that the cloud heights improve further with the addition of the 6.7um fusion channel. What is interesting about this is that the 6.7-µm channel is not generally used for global operational cloud height retrievals; the 13.3-µm channel is more often used. The 6.7-µm channel is strongly impacted by the presence of water vapor, and obviously the amount of water vapor is quite small in the Antarctic. We need to do further study to determine the information content of this channel at high latitudes.**

# Improvement in cloud retrievals from VIIRS through the use of infrared absorption channels constructed from VIIRS-CrIS data fusion

Yue Li[1], Bryan A. Baum[2], Andrew K. Heidinger[3], W. Paul Menzel[1], Elisabeth Weisz[1]

[1]Cooperative Institute for Meteorological Satellite Studies, University of Wisconsin-Madison, Madison, Wisconsin, USA
[2]Science and Technology Corporation, Madison, Wisconsin, USA
[3]NOAA/NESDIS/Center for Satellite Applications and Research, Madison, Wisconsin, USA

*Correspondence to*: Yue Li (yue.li@ssec.wisc.edu)

**Abstract**. Retrieval of semitransparent ice cloud properties from the Visible Infrared Imaging Radiometer Suite (VIIRS) satellite sensor on the Suomi-NPP and NOAA-20 platforms is challenging due to the absence of infrared (IR) water vapor and $CO_2$ absorption channels. However, on these platforms, there is a companion sensor called the Crosstrack Infrared Sounder (CrIS) that provides these spectral measurements, but at a lower spatial resolution (~15 km at nadir). To mitigate the lack of VIIRS spectral measurements in these IR absorption channels, recent studies suggest an approach to supplement VIIRS measurements by fusion of the imager and sounder data. In particular, Weisz et al. (2017) demonstrate a method to construct IR water vapor and $CO_2$ absorption channel radiances for VIIRS at 750m spatial resolution. Based on these constructed channels for both Suomi-NPP and NOAA-20, this study evaluates three cloud properties – cloud mask, cloud thermodynamic phase, and cloud top height – through comparison to the CALIPSO/CALIOP V4-20 cloud layer products and MODIS Collection 6.1 cloud top products. Each of these cloud properties show improvement with the use of these constructed channel radiances. The major improvement for the cloud mask is found over polar regions, where the correct cloud detection percentage increases due to decrease in missed cloud and/or false detection.

For cloud thermodynamic phase, the ice cloud fraction increases over non-polar regions and the combined liquid water and ice cloud discrimination improves in comparison with CALIPSO. The retrieved cloud top height for semitransparent ice clouds increases over non-polar regions and tends to be closer to the true CALIPSO/CALIOP cloud top height. Moreover, the uncertainty of cloud top height retrievals decreases globally for these clouds.

# 1. Introduction

Current polar-orbiting satellite imager sensors, such as the Visible Infrared Imaging Radiometer Suite (VIIRS) onboard both the Suomi National Polar-orbiting Partnership (S-NPP) and the National Oceanic and Atmospheric Administration-20 (NOAA-20), have many advantages compared to previous generation imagers, such as a wider scanning swath, a pixel size that varies little across the scan, and the addition of a day/night band (DNB). However, the absence of certain thermal infrared (IR) bands makes it challenging to accurately retrieve cloud properties that are dependent on those spectral measurements. For instance, VIIRS does not take measurements in the broad 6.7-µm water vapor band or the 15-µm $CO_2$ band that are useful for both cloud thermodynamic phase and semitransparent ice cloud height retrievals (Baum et al. 2012). The 15-µm channels are used in the $CO_2$ slicing approach that was implemented in the National Aeronautics and Space Administration's (NASA) Moderate Resolution Imaging Spectroradiometer (MODIS) products (Menzel et al., 2008; Baum et al. 2012) and High resolution Infrared Radiometer Sounder (HIRS) products (Menzel et al. 2016). Fortunately, these IR channels are available on the hyperspectral IR sensor called the Crosstrack Infrared Sounder (CrIS), also on the S-NPP and NOAA-20 platforms. In general, a sounding sensor is used for retrieving accurate atmospheric temperature and moisture profiles based on its hyperspectral coverage but at a lower spatial resolution than an imager such as VIIRS. CrIS takes measurements at 1305 wavelengths from 3.92-µm to 15.38-µm. The products from the CrIS sounder show significant enhancement over NOAA's legacy HIRS sensors.

Previous studies detected the presence of clouds and retrieved cloud top height directly from sounder data (Masiello et al. 2002, 2003; Susskind et al. 2003; Li et al. 2005; Kahn et al. 2007) but as noted above, the spatial resolution of the sounder is much lower than that of the companion imager. Heidinger et al. (2019) developed a method to match sounder fields-of-view (FOVs; 15-km spatial resolution at nadir) and VIIRS imager pixels (750m at nadir), and adopted the ice cloud top height retrieval from the sounder as the a-priori value to improve the imager-based cloud height retrieval using an optimal estimation approach. Here we denote field-of-view for the sounder and pixel for the imager exclusively to minimize confusion between the two sensors. This method has the advantage of using sounder information as an aid to retrieve products at imager resolution. There are three drawbacks to this approach: (1) both the imager and sounder data need to be available during operational processing, (2) the algorithm must account for spatial gaps between sounder FOVs and the "stretching" of the FOVs towards the edge of the sounder scan swath, and (3) the sounder swath does not cover the entire imager swath.

To mitigate some of these limitations, this study employs an innovative data fusion approach (Weisz et al. 2017) that constructs MODIS-like water vapor and $CO_2$ channel radiances directly at the imager resolution through use of VIIRS and CrIS radiances. To be clear, the data fusion method provides MODIS-like IR absorption channel radiances at the VIIRS M-band spatial resolution

(750m). The VIIRS+CrIS fusion channel radiance products are available for the entire record of both S-NPP and NOAA-20 platforms, and access to these products is described in the Appendix.

The addition of these channels makes it possible to retrieve cloud properties, including cloud mask, cloud type/phase, and cloud top height products using algorithms developed and tested using the full MODIS channel suite. The goal of this study is to determine the impact of supplementing VIIRS with the imager-resolution VIIRS-CrIS fusion channels on retrieving those three cloud products. This paper is organized as follows: Section 2 discusses data and retrieval methods; Section 3 presents results and findings, and a summary is provided in Section 4.

# 2. Data and Data Processing System

## 2.1 VIIRS Level-1 and Level-2 Data

The data used in this study include the standard Level–1B VIIRS data for both the S-NPP and NOAA-20 platforms made available by the Atmosphere Science Investigator-led Processing System (A-SIPS) located at the University of Wisconsin–Madison Space Science Engineering Center (SSEC). Only the M-band moderate spatial resolution (750m) VIIRS Level–1b data are used in this study.

The VIIRS+CrIS IR channel radiances are available in a Level-2 product for the entire records of S-NPP and NOAA-20. A brief summary of the construction of high spatial resolution IR narrowband radiances is as follows. The method requires an accurate colocation between the high spatial resolution imager data (for VIIRS, M-band data are at 750m) and the lower-spatial-resolution sounder data (for CrIS, about 15 km). The fusion method consists of two steps: (a) performing a nearest neighbor search using a k-d tree algorithm on both high spatial (M-band data) and low spatial (M-band data averaged over the CrIS FOV) resolution split-window (11 and 12-µm) imager radiances, and (b) averaging the convolved sounder radiances at low spatial resolution for the five nearest neighbors selected in the previous step for each imager pixel. The term "convolved sounder radiances" refers to the process of applying a given spectral response function (SRF) to the sounder hyperspectral radiances. The fusion product uses SRFs defined for the MODIS sensor on the NASA Earth Observation system (EOS) Aqua platform. Details on the data fusion methodology are in Weisz et al. (2017). The fusion products are available at the Level 1 and Atmosphere Archive and Distribution System (LAADS) Distributed Active Archive Center (DAAC) at NASA Goddard Space Flight Center. The Appendix provides information related to documentation and access to this product.

## 2.2 CLAVR-x

The CLouds from AVHRR-Extended (CLAVR-x) processing system is used to retrieve cloud properties in this study. CLAVR-x is the operational processing system for the Advanced Very High Resolution Radiometer (AVHRR) on NOAA's Polar Operational Environmental Satellites (POES) sensors. The Pathfinder Atmospheres Extended (PATMOS-x) is a climate dataset generated from CLAVR-x (Heidinger et al. 2014). Over time, CLAVR-x has become the development testbed for many of NOAA's operational cloud property retrieval algorithms using a variety of polar-orbiting and geostationary imagers, including the cloud mask (Heidinger et al. 2012), cloud top properties (Heidinger et al. 2019), Daytime Cloud Optical and Microphysical Properties (DCOMP; Walther and Heidinger 2012), cloud cover layer, and cloud base properties

(Noh et al. 2017). Both daytime and nighttime cloud properties are retrieved within CLAVR-x except DCOMP, which uses reflectance channels only. CLAVR-x is available for public use and a user manual is available from the following website: http://cimss.ssec.wisc.edu/clavrx/documentation.html.

The Cloud Mask retrieval algorithm is based on a Naive Bayesian approach (Heidinger et al. 2012). The algorithm uses a combination of visible (VIS: $0.4 < \lambda < 0.75$ μm), near-infrared (NIR: $0.75 < \lambda < 1.1$ μm), shortwave-infrared (SWIR: $1.1 < \lambda < 3$ μm), midwave-infrared (MWIR: $3 < \lambda < 5$ μm), and longwave-infrared (LWIR: $5 < \lambda < 15$ μm) channels to compute cloud probability based on a number of cloud tests for each pixel, and generates a 4-level cloud mask that classifies the pixel as cloudy, probably cloudy, probably clear and clear. In subsequent retrievals and validations, the pixel is considered cloudy if the 4-level mask shows cloudy or probably cloudy; otherwise, the pixel is declared clear. Cloud product retrievals are performed only on cloudy pixels.

The cloud type/phase retrieval is a critical part of the CLAVR-x system. It is based on a traditional decision tree method that uses measurements from the 1.61, 3.75, 8.5, 11 and 12-μm channels. If available, the 6.7 and 13.3-μm channels are also used for cloud thermodynamic phase retrievals, where they primarily impact the discrimination of semitransparent ice clouds.

Cloud top heights are retrieved with the GOES Algorithm Working Group (AWG) Cloud Height Algorithm (ACHA). Details on ACHA are provided in its Algorithm Theoretical Basis Document (ATBD; accessible from http://cimss.ssec.wisc.edu/clavrx/documentation.html). ACHA employs an optimal estimation (OE) algorithm that uses LWIR channels only. ACHA derives the a-priori values based on cloud phase for its cloud top retrieval, so its performance relies on the phase algorithm. Also, ACHA does not process pixels sequentially. Instead, ACHA generates processing paths based on cloud phase, local radiative center (LRC), and multilayer cloud detection. Here the use of LRC allows the algorithm to mitigate complexities arising from pixels having a very low cloud signal, such as cloud edges and optically thin ice clouds; it is defined as the pixel location, in the direction of the gradient vector of brightness temperature at 11 µm, upon which the gradient reverses or when a threshold value is found. Cloudy pixels are assigned into different groups and processed based on group priority. Optically thin ice cloud pixels are processed in the final step using mean retrieved cloud top temperature from surrounding optically thicker ice cloud pixels as the a-priori values.

Table 1 lists the channels used by the cloud mask, cloud type/phase and ACHA cloud top height algorithms, both with and without fusion channels. As shown in Table 1, the fusion water vapor channel at 6.7 µm can be used by both cloud mask and cloud type. The 13.3-µm channel is used in the cloud type and ACHA modules but not in the cloud mask. The reason for this is that the 6.7-µm channel provides the same information as does the 13.3-µm channel; both are not necessary. The ACHA algorithm is versatile in that it supports various combinations of IR channels. Two combinations are tested in this study: one in which only the 13.3-µm fusion channel is added to the VIIRS 8.5, 11, and 12 µm channels, and one in which both the 6.7 and 13.3 µm channels are used in conjunction with the 8.5, 11, and 12 µm channels. Previous studies explored spectral band information useful for cloud property retrievals by computing the Shannon information content (L'Ecuyer et al. 2006; Wang et al. 2016). The approach used here is to test their impact on ice cloud height retrievals through comparison with another cloud height product. In this study, the comparisons are based on both the CALIPSO/CALIOP V4-20 cloud layer products and the MODIS Collection 6.1 cloud top products; these products are described in the following section.

| | No Fusion (µm) | Fusion (µm) |
|---|---|---|
| Cloud Mask | 0.41, 0.65, 0.87, 1.61, 2.25, 3.7, 8.5, 11, 12 | 0.41, 0.65, 0.87, 1.61, 2.25, 3.7, 8.5, 11, 12, 6.7 |
| Cloud Phase | 1.61, 3.7, 8.5, 11, 12 | 1.61, 3.7, 8.5, 11, 12, 6.7, 13.3 |
| ACHA | 8.5, 11, 12 | 8.5, 11, 12, 6.7*, 13.3 |

Table 1. Spectral channels used in the retrievals for fusion and no fusion experiments. The asterisk indicates that we present ACHA results with and without the 6.7-µm channel (results are without 6.7-µm unless inclusion is noted).

## 2.3 Comparison Datasets

The Cloud-Aerosol Lidar with Orthogonal Polarization (CALIOP) instrument is a near-nadir viewing lidar system onboard the Cloud-Aerosol Lidar and Infrared Pathfinder Satellite Observations (CALIPSO; Winker et al. 2009). CALIOP sends active lidar signals downward which can penetrate the atmospheric layers and provide vertical profiles of clouds and aerosols. CALIPSO was part of NASA's A-Train constellation from 2006 until 2018, when it left the A-train for a lower orbit to stay in sync with CloudSat. However, it continues to provide reliable global observations. The orbits of CALIPSO/CALIOP overlap with both S-NPP and NOAA-20 periodically. Over time, the orbits coincide enough to provide global coverage. The CALIPSO products offer a unique assessment of VIIRS cloud retrievals.

In this study, collocations with CALIPSO/CALIOP are studied for two weeks of S-NPP data from April and October 2018 and one week of NOAA-20 data from January 2019. Collocations with CALIPSO are selected as described in Heidinger et al. (2019). Briefly summarized, the time difference must be within 15 minutes between VIIRS and CALIPSO and the spatial distance must be within 4° (great circle latitude and longitude differences). This approach allows maximum collocations between the two sensors, particularly in the polar regions. Though a large spatial distance is used, nearly all collocations (>99% globally) occur within 0.5° and about 60% of collocations are within 0.1°. We also note that use of tighter temporal and spatial thresholds does not impact the results significantly. To make use of the full potential of CALIPSO/CALIOP data, the 1-km and 5-km products are combined when clouds are not reported in the 5-km product. While both Version 3 and 4 CALIPSO/CALIOP products are available, the latest Version 4-20 cloud layer product is used (Vaughan et al., 2018; Avery et al., 2019). In this paper, the true CALIPSO/CALIOP cloud top height for the uppermost cloud layer is used for validation instead of an adjusted CALIPSO/CALIOP cloud top height as described in Heidinger et al. (2019).

The Aqua-MODIS Collection 6.1 (C6.1) cloud height products are used as an additional comparison dataset. Cloud top heights in C6.1 are retrieved with the $CO_2$ slicing technique that uses a combination of $CO_2$ absorption bands (Menzel et al. 2008). Key features of cloud top property refinements for Collection 6 are described in Baum et al. (2012). The collocation tools developed by the Atmosphere SIPS are used to generate collocations between S-NPP/NOAA-20 and Aqua.

# 3. Results

## 3.1 Cloud Mask

Cloud mask retrievals are compared to collocated CALIPSO/CALIOP, with results presented in Table 2. In assessing the cloud mask product, the CALIPSO/CALIOP cloud fraction is used to classify the pixel as to its cloud/clear state. When a cloud layer is detected by CALIPSO/CALIOP, the pixel is classified as cloudy. Neighboring pixels along the path are included and the cloud fraction is defined by computing the ratio between the number of cloudy pixels and the total number of pixels. A cloud fraction of 1 means it is cloudy, and a fraction of 0 implies that the pixel is clear. Pixels with values in between are discarded to avoid cloud edges and the potential for partially-cloudy pixels. Additionally, pixels with CALIPSO/CALIOP cloud optical thickness lower than 0.03 are filtered to exclude sub-visible clouds from the perspective of VIIRS. The fraction of the sub-visible clouds is less than 4% from a global perspective and less than 3% in the polar regions. Table 2 shows the sample sizes and percentages of correct, missed and false detected clouds for different geographical regions for S-NPP and NOAA-20, where a correct detection means that the pixel is classified as cloudy by both VIIRS and CALIPSO/CALIOP. If VIIRS reports clear and CALIOP indicates cloudy, it is classified as a missed cloud. If VIIRS reports cloudy and CALIOP reports clear, the classification is regarded as a false cloud.

From a global perspective, adding a fusion channel tends to increase the correct overall detection percentage and decrease both missed and false cloud percentages. This applies to both platforms and the impact appears to be slightly better for NOAA-20 (from 81.7% to 82.8%) than S-NPP (from 82.5% to 83.3%). A regional analysis indicates that the increase in correct detections occurs primarily over polar regions. The most pronounced change is over the Arctic in the NOAA-20 product, which shows that correct detection increases from 61.9% to 67.6% and the false detection decreases from 13.7% to 7.4%. Unlike S-NPP, results of NOAA-20 do not always show improvement in missed cloud and false detection, which is likely due to differences in orbits, observation geometry, sensor characteristics, etc. Cloud detection over snow-covered surfaces is a challenging problem, and the overall increase of correct detection clearly demonstrates the positive impact of the fusion channels. Over nonpolar regions, a slight increase of correct detection of 0.2 is seen for both platforms. This is unsurprising since the cloud mask algorithm performs fairly well for a snow-free surface even without the water vapor channel. The general conclusion does not change when the optical thickness threshold is changed and when daytime and nighttime is studied separately; the improvement in cloud detection is always observed. This indicates that inclusion of the fusion channel is valuable for cloud detection in problematic regions, without causing negative impacts in other regions. In terms of total cloud fraction, as expected, VIIRS tends to report a lower cloud fraction than CALIOP. CALIOP has a better detection sensitivity to optically thin clouds, and global cloud fractions reported from the two sensors are in agreement when the minimum cloud optical thickness is set between 0.6 and 0.7. The global values do not necessarily become more closely aligned with CALIOP when a fusion channel is used. However, the use of a fusion channel results in a much larger impact in the polar regions, as will be shown in Figure 1.

| | Sample Size | | Correct Detection | Missed Cloud | False Detection | CALIOP Cloud Fraction | VIIRS Cloud Fraction |
|---|---|---|---|---|---|---|---|
| Global | 5873247 | Fusion | 83.3 | 12.5 | 4.2 | 71.9 | 63.7 |
| | | No Fusion | 82.5 | 12.8 | 4.7 | | 63.8 |
| 60°N to 60°S | 4207459 | Fusion | 85.8 | 10.7 | 3.5 | 71.2 | 64.2 |
| | | No Fusion | 85.6 | 10.8 | 3.6 | | 64.1 |
| Arctic | 836038 | Fusion | 76.9 | 15.4 | 7.6 | 72.6 | 64.9 |
| | | No Fusion | 74.7 | 16.8 | 8.4 | | 64.3 |
| Antarctic | 829750 | Fusion | 77.2 | 18.5 | 4.3 | 74.6 | 60.4 |
| | | No Fusion | 74.7 | 19.1 | 6.2 | | 61.8 |

Table 2a. Validation of S-NPP cloud mask detection against CALIPSO/CALIOP using data collocated globally. Data with cloud optical thickness less than 0.03 are filtered out.

| | Sample Size | | Correct Detection | Missed Cloud | False Detection | CALIOP Cloud Fraction | VIIRS Cloud Fraction |
|---|---|---|---|---|---|---|---|
| Global | 2254727 | Fusion | 82.8 | 13.1 | 4.1 | 70.7 | 61.9 |
| | | No Fusion | 81.7 | 13.3 | 5.0 | | 62.6 |
| 60°N to 60°S | 1586709 | Fusion | 85.5 | 10.7 | 3.8 | 72.5 | 65.7 |
| | | No Fusion | 85.3 | 10.8 | 3.9 | | 65.7 |
| Arctic | 319328 | Fusion | 67.6 | 25.0 | 7.4 | 66.4 | 48.8 |
| | | No Fusion | 61.9 | 24.4 | 13.7 | | 55.8 |
| Antarctic | 348690 | Fusion | 84.4 | 12.9 | 2.7 | 66.6 | 56.4 |
| | | No Fusion | 83.3 | 14.4 | 2.3 | | 54.5 |

Table 2b. Validation of NOAA-20 cloud mask detection against CALIPSO/CALIOP using data collocated globally. Data with cloud optical thickness less than 0.03 are filtered out.

Figure 1 shows the global cloud fraction averaged over the study period. Consistent with Table 2, the difference plots show that false cloud detection exists in polar regions in S-NPP in both hemispheres. There is also substantial false cloud detection in the NOAA-20 products over the Arctic. Additionally, missed clouds (VIIRS reports clear and CALIOP indicates cloudy) are prevalent over the Antarctic in the NOAA-20 product, as shown in Table 2.

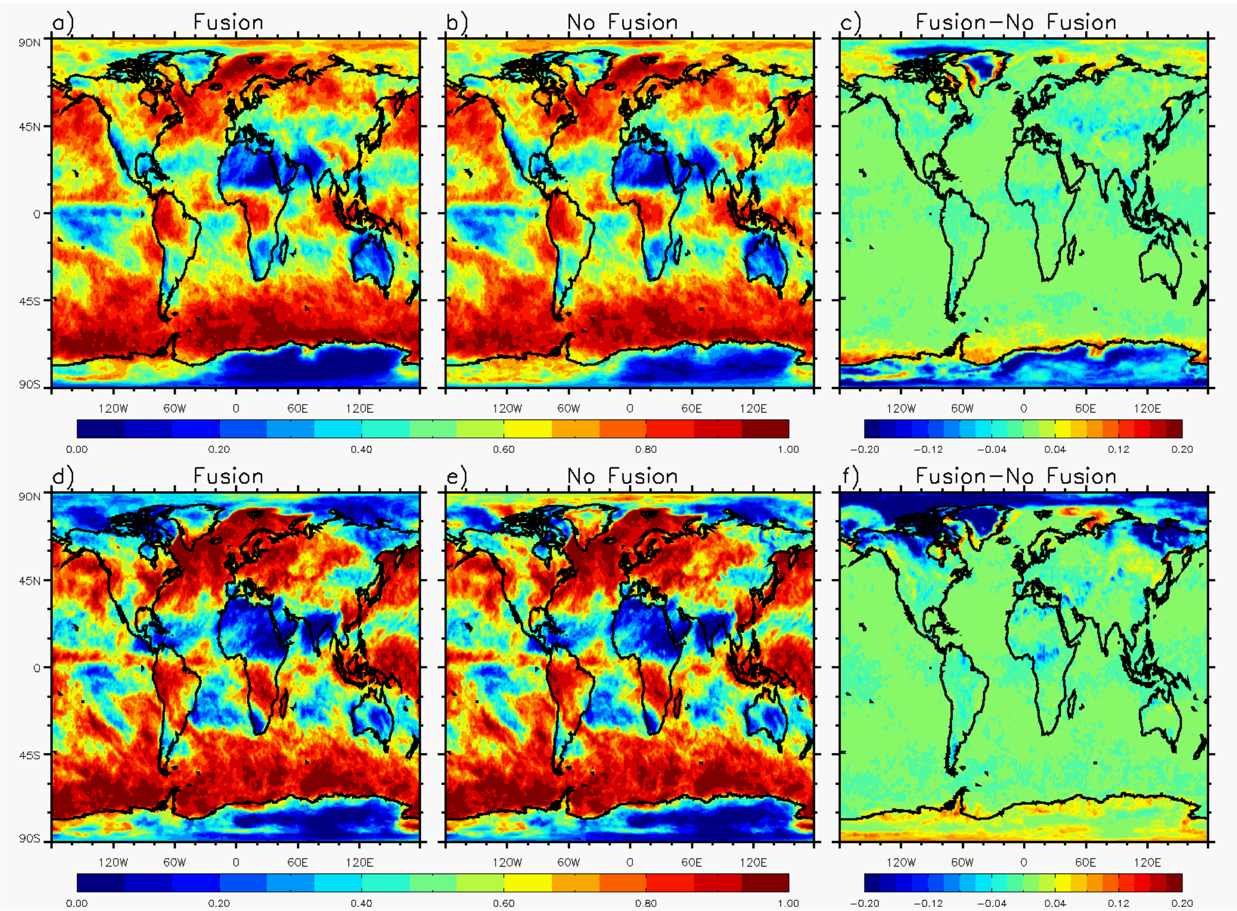

Figure 1. Mean gridded cloud fraction with fusion channels (left column), without fusion channels (middle column) and differences between fusion and no fusion (right column). The upper row shows S-NPP and lower row shows NOAA-20.

## 3.2 Cloud Phase

Misidentification of the cloud phase (i.e., retrieving liquid water clouds as ice phase, and vice versa) directly affects ACHA as it relies on accurate cloud phase discrimination. CLAVR-x uses both the 6.7µm and 13.3µm channels, if available, in its cloud type retrieval algorithm. Table 3 demonstrates the impact of the fusion channels by comparing VIIRS-retrieved cloud phase to CALIPSO/CALIOP. The percentages of both correctly identified and incorrectly identified cloud phase pixels are shown. The total of all four categories adds up to 100%. The percentage of correct identifications for the ice category increases by about 2% for both S-NPP and NOAA-20 when fusion channels are included. However, it also reveals that adding fusion channels tends to slightly decrease the correct identification of liquid water cloud pixels by about 1.5%. Due to the additional water cloud test by the 1.61µm channel when available, more water clouds are detected at daytime (not shown). This also results in slightly larger increase in the percentage of correctly identified ice phase clouds compared to nighttime when fusion channels are used.

| | | | CALIPSO/CALIOP | |
|---|---|---|---|---|
| | | | Ice | Water |
| S-NPP | Fusion | Ice | 39.4 | 4.5 |
| | | Water | 19.3 | 36.8 |
| | No Fusion | Ice | 36.0 | 3.6 |
| | | Water | 22.2 | 38.2 |
| NOAA-20 | Fusion | Ice | 39.8 | 5.3 |
| | | Water | 15.7 | 39.2 |
| | No Fusion | Ice | 36.9 | 4.3 |
| | | Water | 18.1 | 40.7 |

Table 3. Percentages (%) of global cloud phase detection when a valid CTH retrieval is available comparing CALIPSO/CALIOP and CLAVR-x S-NPP VIIRS under both fusion and no-fusion cases.

A geographical distribution plot similar to Figure 1, but for ice cloud only, is shown in Figure 2. The difference plots for both platforms are generally consistent with that in Figure 1. Polar clouds tend to have a high occurrence of ice particles near cloud top, so changes in total cloud fraction over the polar regions are also seen in the ice cloud fraction. This is confirmed by examining the water cloud fractions which show relatively subtle changes from the addition of the fusion channels (not shown). An increase in ice cloud fraction is observed in other regions too, though changes in total cloud fraction are subtle.

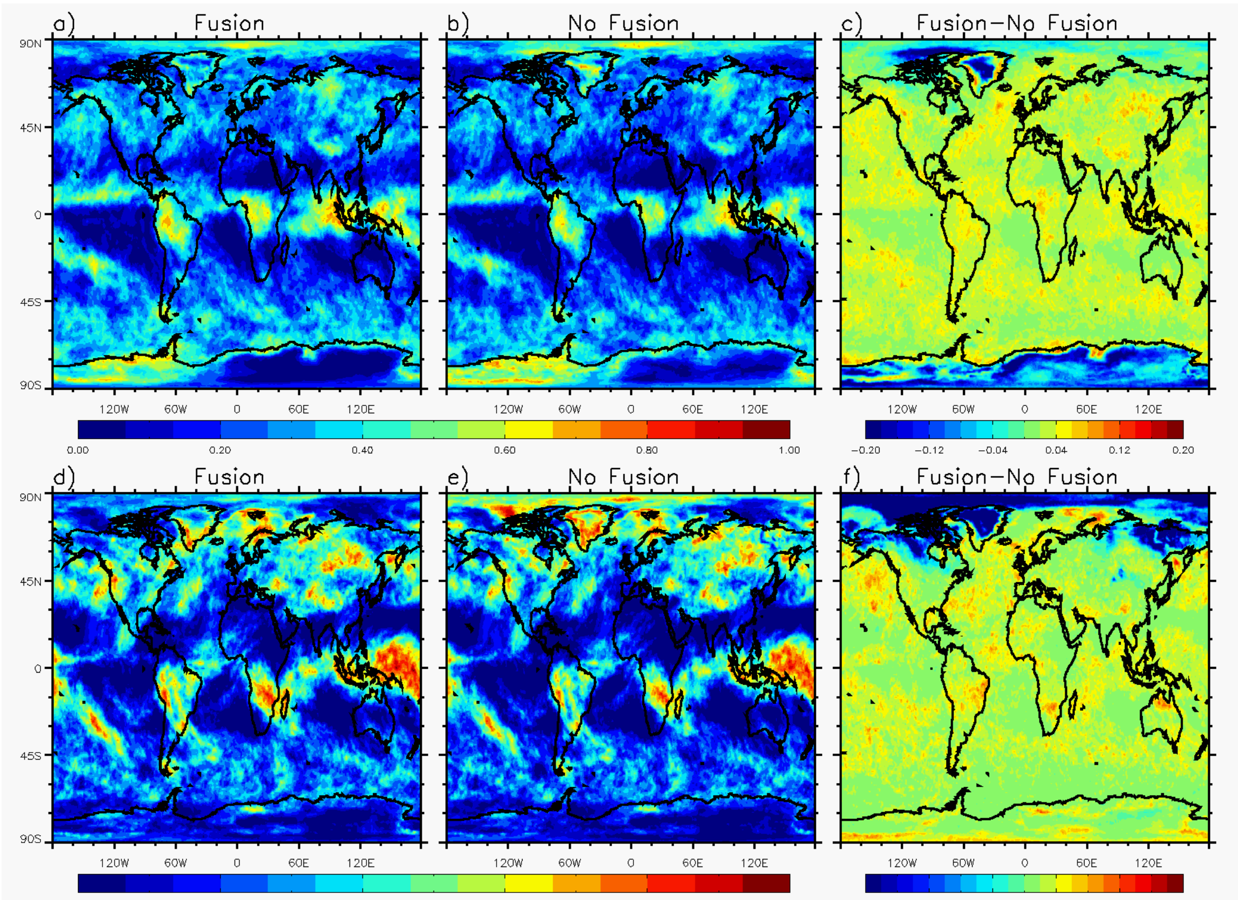


Figure 2. Mean gridded ice cloud fraction with fusion channels (left column), without fusion channels (middle column) and differences between fusion and no fusion (right column). The upper row shows S-NPP and lower row shows NOAA-20.

## 3.3 Cloud Top Height

In the assessment of cloud top height, similar analyses are conducted as in Heidinger et al. (2019). However, as noted earlier, one major difference in this study is the use of the true CALIPSO/CALIOP cloud top instead of the adjusted value. The IR cloud top retrieval inevitably is lower compared to the lidar height. Figure 3 shows an image of 11μm brightness temperatures from S-NPP VIIRS and cloud top height retrievals from MODIS C6.1, and S-NPP VIIRS with and without fusion over the tropical Pacific. Only results for ice clouds are shown. Compared to MODIS, semitransparent ice cloud heights are significantly underestimated using VIIRS channels only (Figure 3c). Figure 3d shows that using the additional information provided by the fusion 13.3um channel improves the retrieval and brings results closer to MODIS C6.1. This clearly shows that ACHA's optimal estimation approach benefits from the fusion channel information.

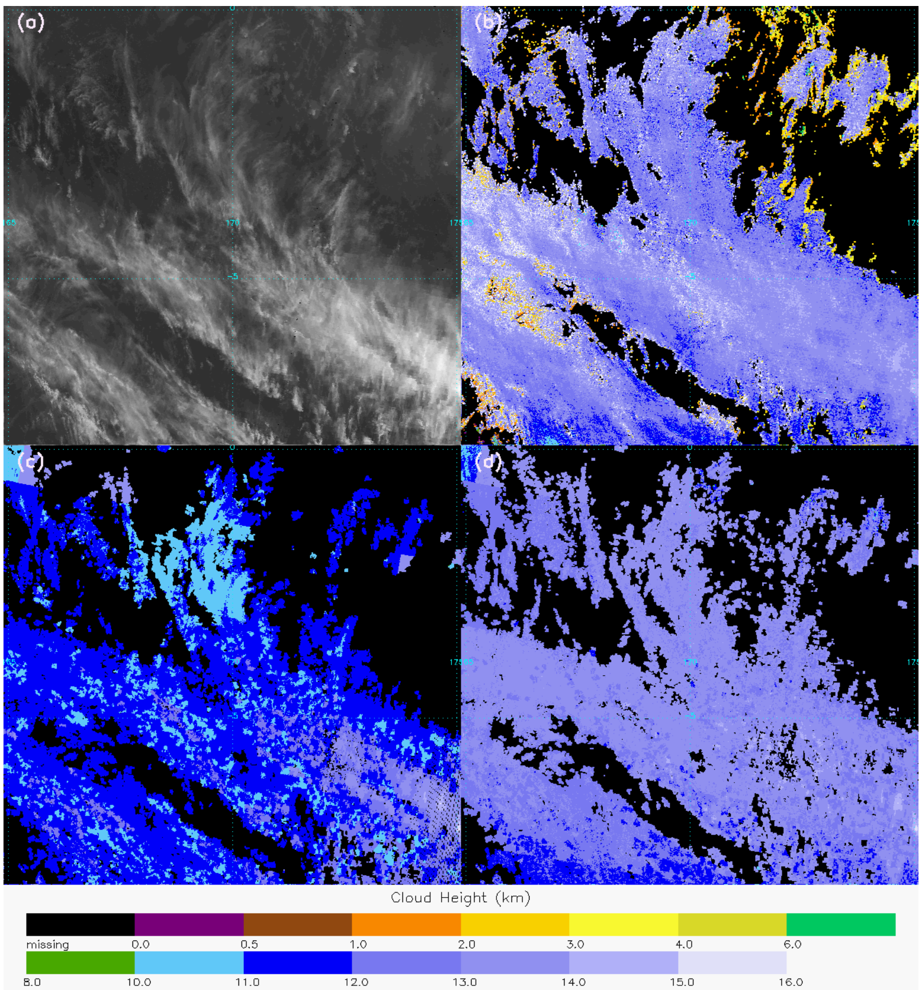


Figure 3. A cirrus cloud scene over tropical Pacific showing a) brightness temperature from S-NPP VIIRS, b) MODIS C6.1, c) no fusion VIIRS, and d) fusion cloud top height for ice clouds only.

Figure 4 plots the histogram of cloud top height bias of ice phase clouds in comparison to CALIPSO/CALIOP for different cloud emissivity ranges for S-NPP VIIRS. Only single layer clouds as reported by CALIPSO/CALIOP are included and both cloud phase and emissivity are matched for each product. As expected, the passive IR-based cloud top height retrieval is lower than in the lidar product. The largest bias is seen for the group with the lowest emissivity. Cloud heights based solely on the VIIRS IR window channels shows that there is a significant fraction of ice clouds that shows negative biases greater than 4km in the two groups with smaller emissivity ranges (Figure 4a and 4b). The retrievals improve significantly if the fusion 13.3-µm channel is used. For optically thicker ice clouds (emissivity between 0.8 to 1.0), the performances from both retrievals are similar as window channels do fairly well for optically thick clouds. In general, when all ice clouds are considered (Figure 4d), the improvement is still quite apparent.

In Figure 5, the zonal means of the cloud top height biases are plotted for different emissivity ranges. The noticeable feature is a dramatic improvement over tropical regions when the emissivity is less than 0.8 (Figs. 5a and 5b), where semitransparent ice clouds are the most prevalent and the underestimation occurs the most frequently. The impact for high latitude regions is generally negligible.

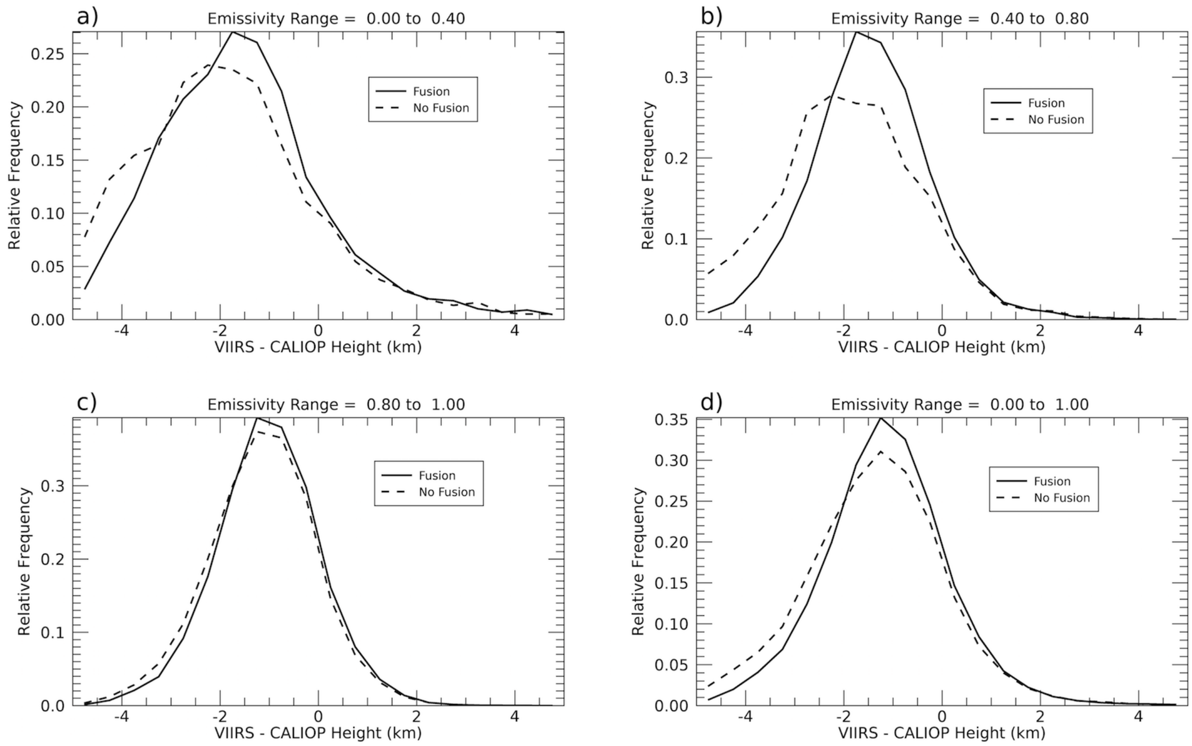


Figure 4. Bias distribution of cloud top height between S-NPP VIIRS and CALIPSO/CALIOP for emissivity range a) 0 to 0.4; b) 0.4 to 0.8; c) 0.8 to 1.0; and d) 0 to 1.0. Solid and dashed lines indicate data with/without fusion channels.

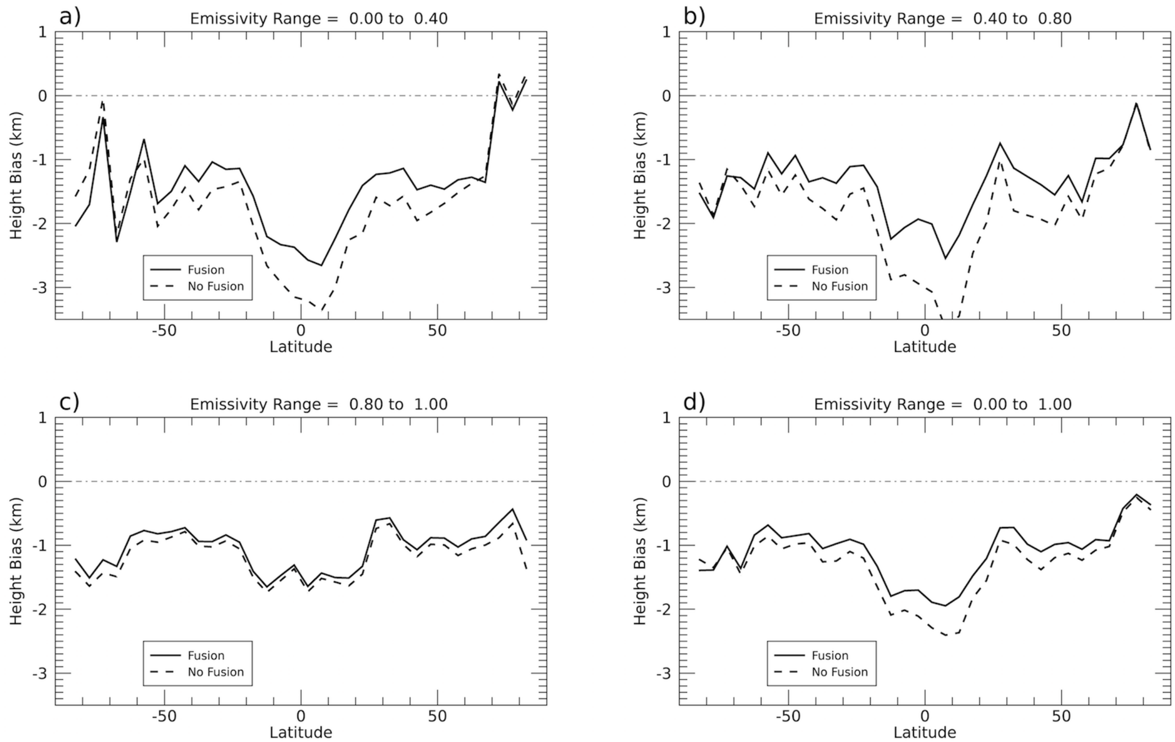


Figure 5. Zonal distribution of cloud height biases between S-NPP VIIRS and CALIPSO/CALIOP for emissivity range a) 0 to 0.4; b) 0.4 to 0.8; c) 0.8 to 1.0; and d) 0 to 1.0. Solid and dashed lines indicate data with/without fusion channels.

Table 4 presents the mean, standard deviation and mode of biases as well as counts of pixels. Not only do the mean biases improve in all cases, but also the standard deviation decreases uniformly. The modes also tend to be closer to 0 except for thick clouds.

| Emissivity | | Counts | Bias (km) | Standard Deviation (km) | Mode (km) |
|---|---|---|---|---|---|
| 0 to 0.4 | No fusion | 62941 | -1.96 | 2.07 | -2.25 |
| | Fusion | | -1.62 | 1.86 | -1.75 |
| 0.4 to 0.8 | No fusion | 22190 | -1.95 | 1.54 | -2.25 |
| | Fusion | | -1.46 | 1.23 | -1.75 |
| 0.8 to 1.0 | No fusion | 227330 | -1.15 | 1.10 | -1.25 |
| | Fusion | | -1.04 | 1.06 | -1.25 |

Table 4. Statistics of differences between S-NPP VIIRS cloud top height and CALIPSO-CALIOP using two weeks of data in April and October in 2018, when fusion/no fusion data are used for four emissivity ranges. Emissivity is from both ACHA and derived from CALIPSO/CALIOP cloud optical thickness.

Similar analyses are also performed on NOAA-20 cloud top height products in Figure 6, Figure 7 and Table 5. It is observed that though the counts in Table 5 are smaller than for S-NPP (since only one rather than two weeks was processed for NOAA-20), positive impacts on cloud top heights are revealed and the performance is consistent between S-NPP and NOAA-20.

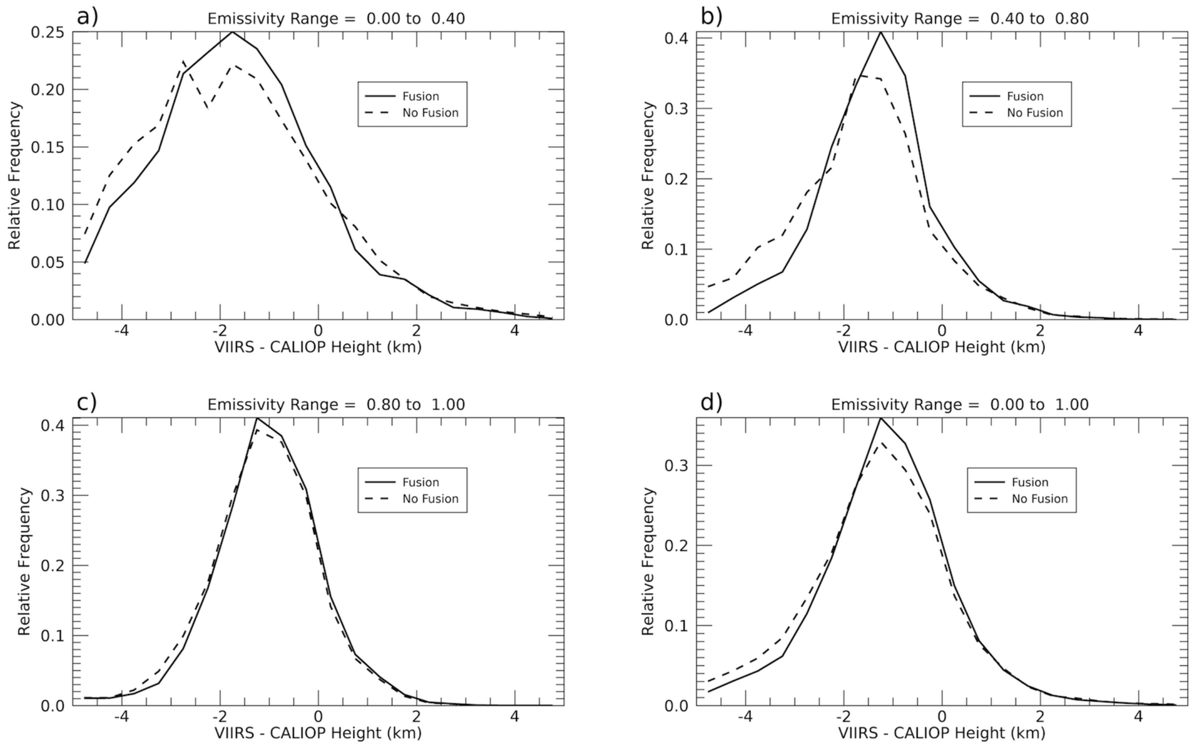


Figure 6. Bias distribution of cloud top height between NOAA-20 VIIRS and CALIPSO/CALIOP for emissivity range a) 0 to 0.4; b) 0.4 to 0.8; c) 0.8 to 1.0; and d) 0 to 1.0. Solid and dashed lines indicate data with/without fusion channels.

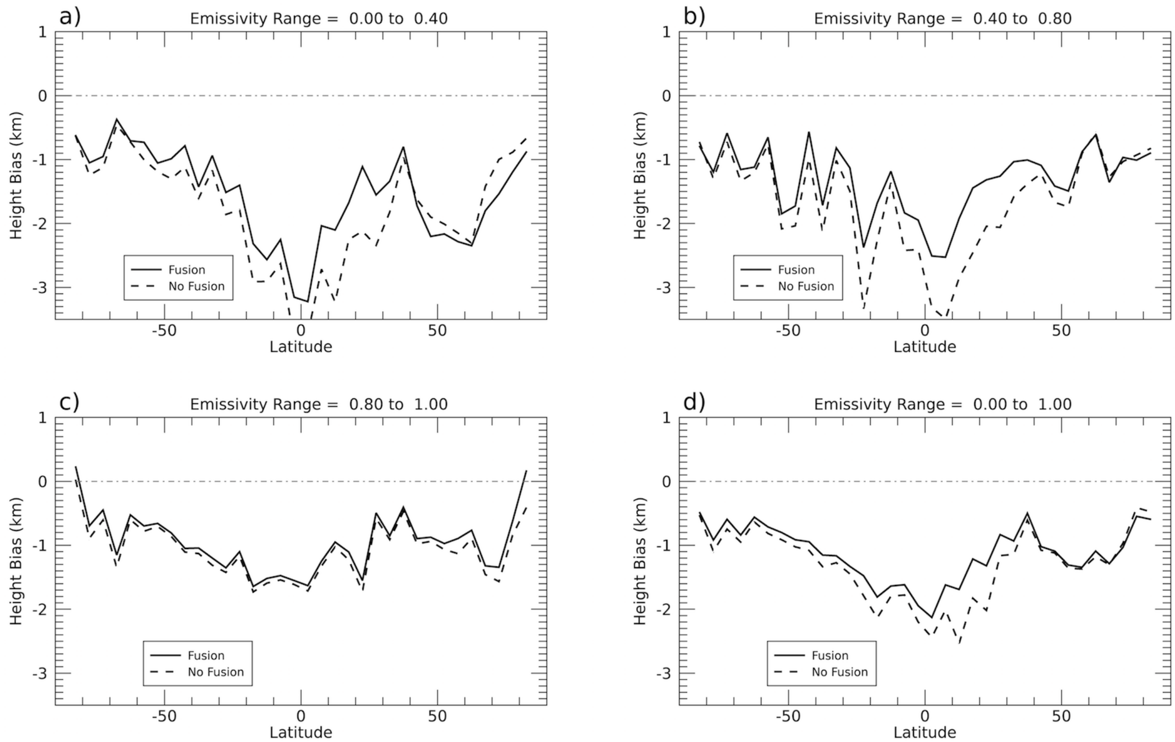


Figure 7. Zonal distribution of cloud height biases between NOAA-20 VIIRS and CALIPSO/CALIOP for emissivity range a) 0 to 0.4; b) 0.4 to 0.8; c) 0.8 to 1.0; and d) 0 to 1.0. Solid and dashed lines indicate data with/without fusion channels.

| Emissivity | | Counts | Bias (km) | Standard Deviation (km) | Mode (km) |
|---|---|---|---|---|---|
| 0 to 0.4 | No fusion | 28875 | -2.02 | 2.07 | -2.75 |
| | Fusion | | -1.83 | 1.85 | -1.75 |
| 0.4 to 0.8 | No fusion | 7192 | -1.78 | 1.51 | -1.75 |
| | Fusion | | -1.37 | 1.19 | -1.25 |
| 0.8 to 1.0 | No fusion | 85079 | -1.12 | 1.12 | -1.25 |
| | Fusion | | -1.03 | 1.09 | -1.25 |

Table 5. Statistics of differences between NOAA-20 VIIRS cloud top retrieval and CALIPSO/CALIOP using one week of data in January 2019, with and without the use of fusion channels for three emissivity ranges.

To demonstrate the impact of fusion water vapor channel on cloud height retrievals, the zonal means of S-NPP cloud top height biases retrieved with both 6.7-µm and 13.3-µm compared to VIIRS-only channels are displayed in Figure 8. Compared to adding only the 13.3-µm fusion channel, cloud heights tend to increase and match more closely to those from CALIPSO/CALIOP. This is observed not only for optically thin clouds with emissivities less than 0.4 but also for clouds in the 0.4 to 0.8 emissivity range. Therefore, the water vapor channel adds to the information available from the 13.3-µm $CO_2$ band. The optimal use of the fusion channels deserves further study.

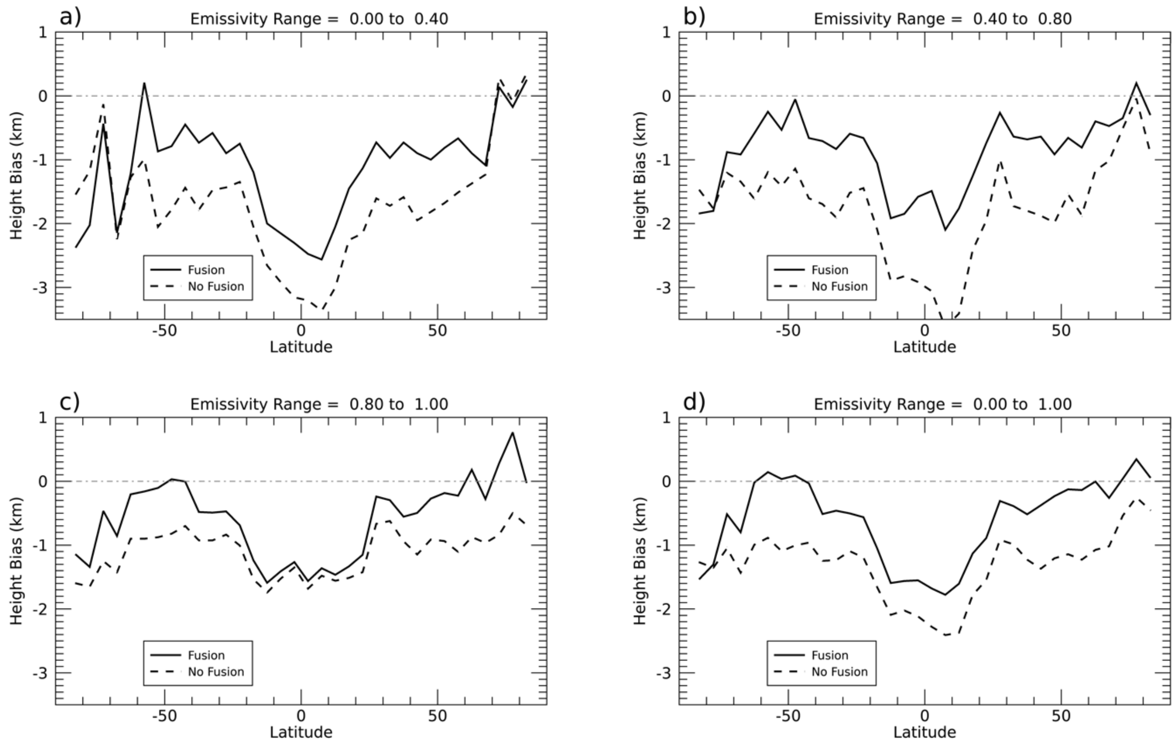


Figure 8. Zonal distribution of cloud height biases between S-NPP VIIRS and CALIPSO/CALIOP for emissivity range a) 0 to 0.4; b) 0.4 to 0.8; c) 0.8 to 1.0; and d) 0 to 1.0. Solid and dashed lines indicate data with/without fusion channels. Both 6.7-µm and 13.3-µm fusion channels are used for the fusion experiment.

While both Heidinger et al. (2019) and this study address the same problem with different approaches involving similar channels from the CrIS sounder, both studies show positive impact when using the sounder channels. However, Heidinger et al. (2019) showed that the major improvement of ice cloud height retrieval was for those in emissivity ranges 0 to 0.4. This study suggests that using the fusion channels may have a greater impact on the ice clouds with emissivity ranges between 0.4 and 0.8.

## 3.4 Cloud Top Height Retrieval Uncertainty

Estimation of retrieval uncertainty is an important output from the optimal estimation approach. The retrieval uncertainty measures the confidence of the retrieval product. A lower uncertainty can be interpreted as there being a higher confidence in the retrieval results, and vice versa. In the optimal estimation output, the retrieval uncertainty is the square root of the diagonal component of the error covariance matrix of the retrievals. ACHA first generates retrieval an uncertainty for each of the retrieved parameters including cloud top temperature, and the uncertainty of cloud top height is derived subsequently by dividing the cloud top temperature uncertainty by a lapse rate. Here a constant lapse rate of 7K/km is used. Figure 9 shows the zonal mean retrieval uncertainty of the ice cloud top heights using global sub-sampled Level 2b data, which are derived at a 0.1˚ by 0.1˚ spatial resolution using a nearest neighbor nadir-overlap sampling technique. Level 2b subsampled data are computed daily from level 2 data separately for ascending and descending tracks. Several features are noticed: 1) the uncertainties are smaller with variations between 1.0km and 1.5km between 60°N and 60°S; 2) the uncertainties increase gradually poleward of 60° and the maximum values are about 0.2km (~2K) at both hemispheres; 3) results using fusion channels reduce uncertainties across all latitudes and the major improvement is between 60°N and 60°S.

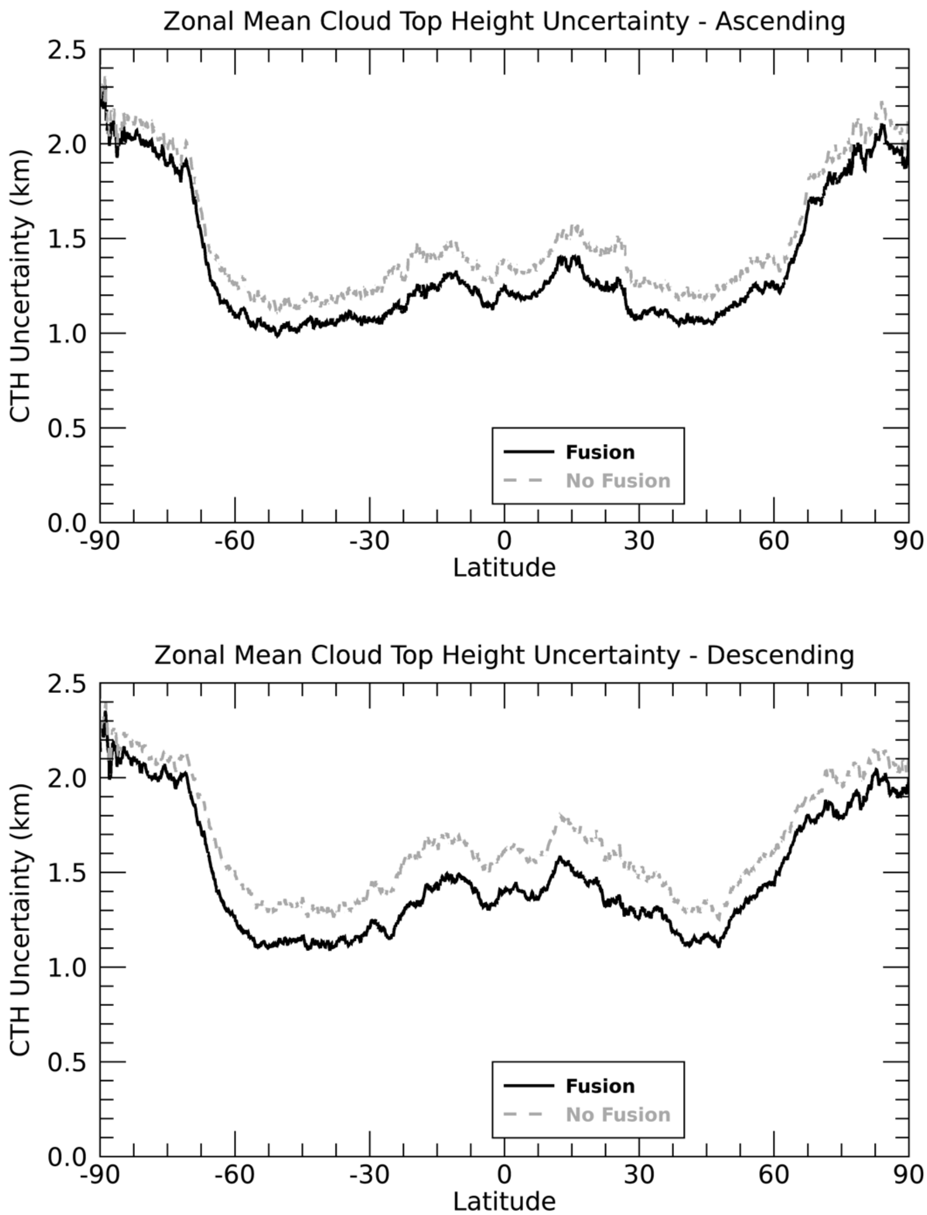


Figure 9. Zonal mean ice cloud top height uncertainty estimated from ACHA's optimal estimation algorithm for S-NPP VIIRS computed from two weeks of global Level 2b data in 2018. The top panel shows the ascending track and the bottom panel shows the descending track.

Figure 10 shows ice cloud top height uncertainty as a function of cloud emissivity, derived from the same global Level 2b data as in Figure 9. Larger differences for ice clouds with smaller emissivities are expected and this result is supported by the results in Figure 10. As emissivity increases above 0.8, the differences tend to decrease gradually. It is also observed that the differences are negligible when emissivity is less than 0.05, which can be explained by the limitation of passive sensors such as VIIRS in detecting such optically thin clouds.

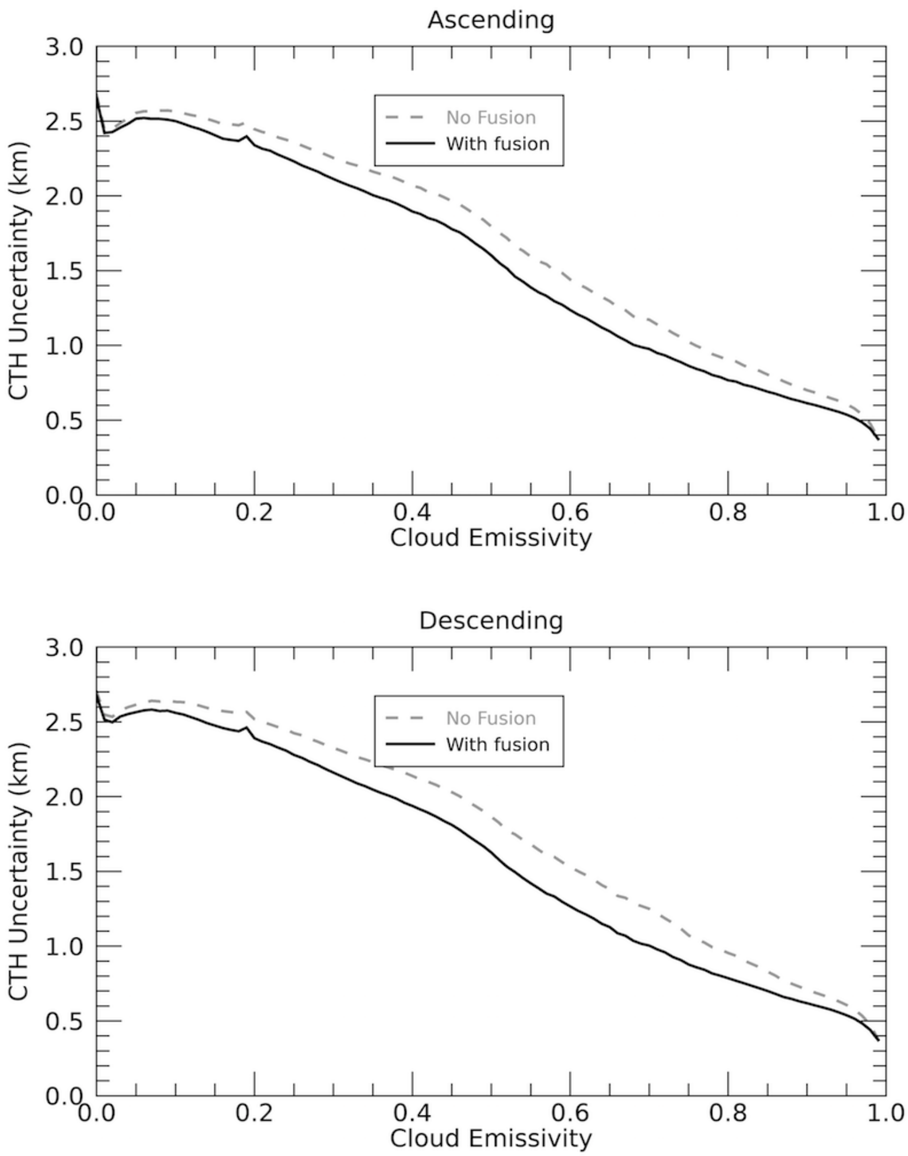


Figure 10. Ice cloud top height uncertainty as a function of cloud emissivity for the S-NPP VIIRS computed from two weeks of global Level 2b data in 2018.

# 4. Summary and Discussion

The absence of water vapor and $CO_2$ absorption IR channels on the VIIRS imager on the Suomi-NPP and NOAA-20 polar-orbiting platforms limits the capability for cloud property retrievals, especially for retrievals involving semitransparent ice clouds. This study shows the advantage of using two IR absorption channels at 6.7 and 13.3 μm that are constructed at VIIRS M-band (moderate band) spatial resolution (750m) using a data fusion approach using both sounder (CrIS) and imager (VIIRS) measurements following Weisz et al. (2017). The positive impact of using the constructed 6.7 and 13.3-μm fusion channels on three cloud properties (cloud mask, type/phase, and cloud top height) is demonstrated. The cloud retrievals are based on the NOAA operational CLouds from AVHRR-extended (CLAVR-x) retrieval package. The cloud height module is called the AWG Cloud Height Algorithm (ACHA), where AWG refers to the Algorithm Working Group set up a number of years ago in preparation for working with data from the GOES Advanced Baseline Imager. Evaluation of the resulting cloud products are performed through comparison to the CALIPSO/CALIOP V4-20 cloud layer products and MODIS Collection 6.1 cloud top products.

We note that improvements are observed for all three products when quantitatively compared to the CALIPSO/CALIOP products. Each of these cloud properties show improvement with the use of one or both of the 6.7 and 13.3-μm fusion channel radiances. The major improvement for cloud mask is over polar regions, where percentage of cloud detection increases due to decrease in missed cloud and/or false cloud detection.

With regard to cloud thermodynamic phase, the ice cloud fraction increases over non-polar regions and the combined detection rates for both water and ice clouds also increase. The impact of using

IR absorption channels in this study are similar to the impact shown in MODIS Collection 6 products that added similar channels to improve the approach in Collection 5 that used only the 8.5, 11, and 12-µm IR window channels (Baum et al. 2012).

The retrieved cloud top height for semitransparent ice clouds increases in non-polar regions and tends to be closer to the true CALIPSO/CALIOP cloud top. The retrievals obtained using the 13.3-µm channel in addition to the 8.5, 11, and 12-µm IR window channels are improved over those obtained solely with the IR window channels. The retrieved semitransparent ice cloud heights are closer to the CALIPSO V4-20 product, and both the biases and standard deviations decrease. The inclusion of a channel at 6.7- µm further decreases the bias and standard deviation values. This suggests that there is room for additional improvement in the cloud height retrievals by testing different combinations of the IR absorption fusion channels. The positive impact on cloud heights, as compared to CALIPSO, is seen at all latitudes for both Suomi-NPP and NOAA-20 platforms, and the uncertainty in the cloud top height retrievals decreases at almost all latitudes.

The approach described in Heidinger et al. (2019) also used a combination of VIIRS and CrIS radiance data to demonstrate the potential for improving ice cloud retrievals. With the data fusion product available for VIIRS, however, the constructed IR absorption channel radiances are provided at VIIRS M-band (750m) spatial resolution for the full imager swath. The fusion results indicate a positive impact in cloud height over a range in emissivity up to 0.8. The results in this study are limited to a VIIRS sensor scan angle of 50˚ to minimize the impact of the sounder swath being less than that of the imager. These findings are limited in scope but clearly demonstrate the potential in the use of the fusion IR absorption channels in generating cloud products. In future work, we plan to extend this evaluation to longer time periods.

**Data availability**. The VIIRS Level-1 data and Level-2 fusion products used in this study were obtained from the A-SIPS data archive (https://sips.ssec.wisc.edu/#/products/list, last access: December 26, 2019). Currently the VIIRS Level-1 and Level-2 fusion data are accessible to the public, free of charge, from the LAADS data center, and more information is provided in the Appendix. The following CALIPSO standard data products were used in this study: the CALIPSO Level-2 1-km cloud layer product V4-20 (Vaughan et al., 2018; NASA Langley Research Center Atmospheric Science Data Center; https://eosweb.larc.nasa.gov/project/calipso/cal_lid_l2_01kmclay-standard-v4-20, last access: December 26, 2019); the CALIPSO Level-2 5-km cloud layer product V4-20 (Vaughan et al., 2018; NASA Langley Research Center Atmospheric Science Data Center; https://eosweb.larc.nasa.gov/project/calipso/cal_lid_l2_05kmclay_standard_v4_20, last access: December 26, 2019). MODIS data comparisons were conducted using the MODIS Collection 6.1 Atmosphere L2 MYD06 Cloud Product (https://ladsweb.modaps.eosdis.nasa.gov/missions-and-measurements/products/MYD06_L2, last access: December 26, 2019)

**Competing Interests**. The authors declare that they have no conflict of interest.

**Author Contributions**. Yue Li conducted the impact study of using fusion channels, performed the analyses and prepared the figures as well as the first draft of the manuscript. Bryan A. Baum and W. Paul Menzel made critical suggestions on the design of the study and significant improvements to the manuscript. Andrew K. Heidinger gave guidance on the use of CLAVR-x and interpretation of results. Elisabeth Weisz provided expertise on the use of fusion products.

**Acknowledgements**. The authors gratefully acknowledge support from NASA grant 80NSSC18K0816 and the encouragement of Dr. Hal Maring (NASA Headquarters, Washington, DC). Yue Li and Andrew K. Heidinger also acknowledge the support from NOAA grant NA15NES4320001. The fusion data are generated by the Atmosphere SIPS at University of Wisconsin – Madison and are available at LAADS (see Appendix). The writing of this paper benefited from discussions with our colleague Denis Botambekov. We thank Geoff Cureton for his effort at the A-SIPS and Bhaskar Ramachandran for help in staging the fusion product at LAADS and providing link to the data.

# Appendix: Accessing the VIIRS+CrIS Fusion Products

The Level-1 and Atmosphere Archive & Distribution System (LAADS) data center manages and hosts VIIRS+CrIS fusion products derived from the Suomi National Polar-orbiting Partnership (S-NPP) and NOAA-20 platforms. The following links provide access to users interested in acquiring these products, which are free of charge. All users need to register with NASA Earthdata to obtain a login account through the NASA User Registration System (URS) page (https://urs.earthdata.nasa.gov). For additional help on any aspect of searching for or acquiring these products, contact the LAADS User Services: http://MODAPSUSO@lists.nasa.gov.

1. **The VIIRS+CrIS Fusion product page (provides overview and documentation):** https://ladsweb.modaps.eosdis.nasa.gov/missions-and-measurements/science-domain/viirs-cris-fusion/
2. **Perform a specific geographical search for the S-NPP VIIRS+CrIS fusion product:** https://ladsweb.modaps.eosdis.nasa.gov/search/order/2/FSNRAD_L2_VIIRS_CRIS_SNPP—5110

3. **Perform a specific geographical search for the NOAA-20 VIIRS+CrIS fusion product:** https://ladsweb.modaps.eosdis.nasa.gov/search/order/2/FSNRAD_L2_VIIRS_CRIS_NOAA20--5110
4. **Direct access to the S-NPP VIIRS+CrIS fusion product archive:** https://ladsweb.modaps.eosdis.nasa.gov/archive/allData/5110/FSNRAD_L2_VIIRS_CRIS_SNPP/
5. **Direct access to the NOAA-20 VIIRS+CrIS fusion product archive:** https://ladsweb.modaps.eosdis.nasa.gov/archive/allData/5110/FSNRAD_L2_VIIRS_CRIS_NOAA20

# References


Avery, M. A., Ryan, R. A., Getzewich, B. J., Vaughan, M. A., Winker, D. M., Hu, Y., Garnier, A., Pelon, J., and Verhappen, C. A.: CALIOP V4 Cloud Thermodynamic Phase Assignment and the Impact of Near-Nadir Viewing Angles, Atmos. Meas. Tech. Discuss., https://doi.org/10.5194/amt-2019-388, in review, 2020.

Baum, B. A**.**, Menzel, W. P., Frey, R. A., Tobin, D., Holz, R. E., Ackerman, S. A., Heidinger, A. K., and Yang, P.: MODIS cloud top property refinements for Collection 6. J. Appl. Meteorol. Clim., 51, 1145-1163, 2012.

Heidinger, A.K.; Evan, A.T.; Foster, M. J., and Walther, A.: A naive Bayesian cloud detection scheme derived from CALIPSO and applied with PATMOS-x. J. Appl. Meteorol. Clim., 51, 1129–1144, 2012.

Heidinger, A. K., Foster, M. J., Walther, A., and Zhao, X.: The Pathfinder Atmospheres-Extended AVHRR climate dataset. B. Am. Meteorol. Soc., 95, 909–922, https://doi.org/10.1175/BAMS-D-12-00246.1, 2014.

Heidinger, A. K., Bearson, N., Foster, M. J., Li, Y., Wanzong, S., Ackerman, S., Holz, R. E., Platnick, S., and Meyer, K.: Using Sounder Data to Improve Cirrus Cloud Height Estimation from Satellite Imagers, J. Atmos. Ocean. Tech., 1331-1342, 2019.

Kahn, B. H., Eldering, A., Braverman, A. J., Fetzer, E. J., Jiang, J. H., Fishbein, E., and Wu, D. L.: Toward the characterization of upper tropospheric clouds using Atmospheric Infrared Sounder and Microwave Limb Sounder observations. J. Geophys. Res., 112, D05202, 2007.

L'Ecuyer, T. S., Gabriel, P., Leesman, K., Cooper, S. J., and Stephens, G. L.: Objective assessment of the information content of visible and infrared radiance measurements for cloud micro hysical property retrievals over the global oceans. Part I: Liquid clouds, J. Appl. Meteorol. Clim, 45, 20–41, 2006.

Li, J., Huang, H.-L., Liu, C.-Y., Yang, P., Schmit, T. J., Wei, H., Weisz, E., Guan, L., and Menzel, W. P.: Retrieval of cloud microphysical properties from MODIS and AIRS. J. Appl. Meteorol., 44, 1526–1543, https://doi.org/10.1175/JAM2281.1, 2005.

Masiello, G., Matricardi, M., Rizzi, R., and Serio, C.: Homomorphism between cloudy and clear spectral radiance in the 800-900-cm$^{-1}$ atmospheric window region. Appl. Opt., 41, 965-973, 2002.

Masiello, G., Serio, C., and Shimoda, H.: Qualifying IMG tropical spectra for clear sky. J. Quant. Spectrosc. Ra., 77/2, 131-148, 2003.

Menzel, W. P., Frey, R. A, Zhang, H., Wylie, D. P., Moeller, C. C., Holz, R. E., Maddux, B., Baum, B. A., Strabala, K. I., and Gumley, L. E.: MODIS global cloud-top pressure and amount estimation: Algorithm description and results. J. Appl. Meteorol. Clim., 47, 1175–1198, https://doi.org/10.1175/2007JAMC1705.1, 2008.

Menzel, W. P., Frey, R. A., Borbas, E. E., Baum, B. A., Cureton, G., and Bearson, N.: Reprocessing of HIRS satellite measurements from 1980 to 2015: Development toward a consistent decadal cloud record. J. Appl. Meteorol. Clim., 55, 2397-2410. doi: 10.1175/JAMC-D-16-0129.1, 2016.

Noh, Y. J., Forsythe, J. M., Miller, S. D., Seaman, C. J., Li, Y., Heidinger, A. K., Lindsey, D. T., Rogers, M. A., and Partain., P. T.: Cloud-Base Height Estimation from VIIRS. Part II: A Statistical Algorithm Based on A-Train Satellite Data. J. Atmos. Ocean. Tech., 34(3), 585-598, 2017.

Susskind, J., Barnet, C. D., and Blaisdell,  J. M.: Retrieval of atmospheric and surface parameters from AIRS/AMSU/HSB data in the presence of clouds. IEEE Trans. Geosci. Remote Sens., 41, 390–409, https://doi.org/10.1109/TGRS.2002.808236, 2003.

Vaughan, M., Pitts, M., Trepte, C., Winker, D., Detweiler, P., Garnier, A., Getzewich, B., Hunt, W., Lambeth, J., Lee, K.-P., Lucker, P., Murray, T., Rodier, S., Tremas, T., Bazureau, A., and Pelon, J.: Cloud-Aerosol LIDAR Infrared Pathfinder Satellite Observations (CALIPSO) data management system data products catalog, Release 4.40, NASA Langley Research Center Document PC-SCI-503, 173 pp., available at: https://www-calipso.larc.nasa.gov/products/CALIPSO_DPC_Rev4x40.pdf (last access: December 2016, 2019), 2018.

Walther, A. and Heidinger, A. K.: Implementation of the Daytime Cloud Optical and Microphysical Properties Algorithm (DCOMP) in PATMOS-x, J. Appl. Meteorol. Clim., 51, 1371–1390, https://doi.org/10.1175/JAMC-D-11-0108.1, 2012.

Wang, C., Platnick, S., Zhang, Z., Meyer, K., and Yang, P.: Retrieval of ice cloud properties using an optimal estimation algorithm and the MODIS infrared observations. Part I: Forward model, error analysis, and information content. J. Geophys. Res., 121, 5809-5826, 2016.

Weisz, E., Baum, B. A., and Menzel, W. P.: Fusion of satellite-based imager and sounder data to construct supplementary high spatial resolution narrowband IR radiances. J. Appl. Remote Sens. 11(3), 036022, doi: 10.1117/1.JRS.11.036022, 2017.

Winker, D. M., Vaughan, M. A., Omar, A., Hu, Y., Powell, K. A. , Liu, Z., Hunt, W. H., and Young, S. A.: Overview of the CALIPSO mission and CALIOP data processing algorithms. J. Atmos. Ocean. Tech., 26, 2310–2323, https://doi.org/10.1175/2009JTECHA1281.1, 2009.